Electro-activated persulfate oxidation of malachite green by boron-doped diamond (BDD) anode: effect of degradation process parameters

Dongtian Miao, Guoshuai Liu, Qiuping Wei, Naixiu Hu, Kuangzhi Zheng, Chengwu Zhu, Ting Liu, Kechao Zhou, Zhiming Yu and Li Ma

ABSTRACT

In this paper, boron-doped diamond (BDD) electro-activated persulfate was studied to decompose malachite green (MG). The degradation results indicate that the decolorization performance of MG for the BDD electro-activated persulfate (BDD-EAP) system is 3.37 times that of BDD electrochemical oxidation (BDD-EO) system, and BDD-EAP system also exhibited an enhanced total organic content (TOC) removal (2.2 times) compared with BDD-EO system. Besides, the degradation parameters such as persulfate concentration, current density, and pH were studied in detail. In a wider range of pH (2–10), the MG can be efficiently removed (>95%) in 0.02 M persulfate solution with a low current density of 1.7 mA/cm^2 after 30 min. The BDD-EAP technology decomposes organic compounds without the diffusion limitation and avoids pH adjustment, which makes the EO treatment of organic wastewater more efficient and more economical.

Key words | BDD, electro-activated, malachite green, organic wastewater, persulfate

Dongtian Miao
Qiuping Wei (corresponding author)
Naixiu Hu
Kuangzhi Zheng
Chengwu Zhu
Ting Liu
Kechao Zhou
Zhiming Yu
Li Ma
State Key Laboratory of Powder Metallurgy,
School of Materials Science and Engineering,
Central South University,
Changsha 410083,
China
E-mail: *qiupwei@csu.edu.cn*

Guoshuai Liu
State Key Laboratory of Urban Water Resource and Environment, School of Environment,
Harbin Institute of Technology,
Harbin 150090,
China

HIGHLIGHTS

- Persulfate is used as a supporting electrolyte to degrade MG.
- An effective electro-activated persulfate (EAP) method was proposed.
- EAP can achieve high degraded efficiency at low current density and low electrolyte concentration.
- EAP can significantly reduce the energy consumption required for degradation relative to other methods.

INTRODUCTION

Water pollution has been a global problem with the increase of industrialization in various countries. A large amount of wastewater, including printing and dyeing wastewater, chemical wastewater, pharmaceutical wastewater, and tannery wastewater, are continuously produced in many industries (Diaz *et al.* 2011; Zhou *et al.* 2011; Katsoni *et al.* 2014; Mei *et al.* 2018a; Siedlecka *et al.* 2018). It is important to find efficient and low-energy demand technologies due to the large refractory sewage emission. Malachite green (MG) is a typical synthetic organic dye and widely used in dyes and fungicides (Srivastava *et al.* 2004; García-Rodríguez *et al.* 2016). MG and its intermediate products are seriously toxic to the water environment because of its biotoxicity and low biodegradability (Perez-Estrada *et al.* 2008; Gopinathan *et al.* 2015; Qu *et al.* 2019). As an emerging effective wastewater treatment technology, electrochemical advanced oxidation processes (EAOPs) can produce a highly oxidizing substance ·OH ($E^0 = 2.7$ V, Vs. standard hydrogen electrode, SHE) by applying an electric potential to the anode (Guenfoud *et al.* 2014; Sasidharan Pillai & Gupta 2016; Ansari & Nematollahi 2018), and the generated hydroxyl radical can decompose the organic compounds efficiently thus leads a high degradation performance (Anglada *et al.* 2011; Chaplin 2014; Flores *et al.* 2017).

doi: 10.2166/wst.2020.176

In recent years, different electrode materials, including graphite, boron-doped diamond (BDD) (Zhou *et al.* 2016), titanium electrodes, and lead oxide have been used to degrade organic sewage with different physical and chemical properties (Fernandes *et al.* 2014; Xing *et al.* 2018; Taner Can *et al.* 2019; Wachter *et al.* 2019). In particular, BDD has been widely used to treat various types of wastewater because of its large potential window and good chemical corrosion resistance (Deng *et al.* 2017; Candia-Onfray *et al.* 2018; Mei *et al.* 2018b; Zhu *et al.* 2018; Zheng *et al.* 2019). The modification of BDD has attracted great attention to improve the specific surface area and change the doping elements to produce hydroxyl radicals effectively (He *et al.* 2015; Mei *et al.* 2019). However, the effective mineralization of organic pollutants is also limited due to the short half-life time of ·OH (10^{-9}s), thus the active radicals can only survive in the surface nearby anode which results in high energy consumption and low degradation efficiency (Haidar *et al.* 2013).

Persulfate is a strong oxidizing reagent ($E^0 = 2.01$ V, SHE) that is close to ozone ($E^0 = 2.07$ V, SHE) (Cao *et al.* 2019; Su *et al.* 2019). Persulfate is relatively stable at room temperature, but it is easily activated under specific external conditions such as ultraviolet, ultrasonic, heat, electricity, and transition metals to produce $\cdot SO_4^-$ (E = 2.5–3.1 V) (Xiong *et al.* 2014; Chen *et al.* 2019a; Gao *et al.* 2019; Hayat *et al.* 2019; Lin *et al.* 2019; Sun *et al.* 2019). $\cdot SO_4^-$ obtained greater oxidizing ability than ·OH in a neutral and alkaline environment. More importantly, compared with ·OH, $\cdot SO_4^-$ has a longer half-life and it can react with organic compounds much easier in bulk solution (Long *et al.* 2019). Amongst the various activation method, electro-activated persulfate technology is more efficient, simpler and does not cause secondary pollution (Matzek & Carter 2016). Combining persulfate activation technology with electrochemical oxidation technology can achieve higher degradation efficiency and reduce power consumption (Carter & Farrell 2008). Some works compared the variety of electrode materials for electroactive persulfate (as: SnO_2, Pt, BDD) and considered that BDD can obtain satisfactory persulfate activation and degradation efficiency (Cai *et al.* 2014; Chen *et al.* 2019b; Ding *et al.* 2019).

Herein, we report our work with decomposing malachite green dye wastewater by BDD electro-activated persulfate (BDD-EAP). Firstly, the BDD anode was successfully prepared by the hot filament chemical vapor deposition (HFCVD) method, and the morphology and structure of BDD were characterized. Secondly, the degradation efficiency and energy consumption of BDD-EAP technology were investigated in detail compared with the traditional BDD-EAP system, and then the optimization of the degradation parameters such as persulfate concentration, current density, and initial pH were developed. Lastly, possible mechanisms for BDD-EAP process were proposed.

EXPERIMENT

The BDD electrode was formed

The BDD electrode used in the experiment was deposited on a 50 mm × 60 mm × 2 mm Si substrate by hot filament chemical vapor deposition (HFCVD) of six straight wires arranged in parallel. The distance between the hot filaments was 10 mm, and the distance from the hot filaments to the substrate was 8 mm. The mixture of gas was in the ratio of B_2H_6 (diluted by 95% of hydrogen): CH_4: $H_2 = 0.6$ sccm (standard-state cubic centimeter per minute) : 4 sccm: 100 sccm. The temperature of the deposition system was kept at 850 °C and the pressure was maintained at 3 kPa, the deposition time was 2 h. The deposition process was later changed to H_2: B_2H_6: CH_4=100 sccm: 3 sccm: 0.45 sccm, deposition time was 10 h, and deposition temperature was 850 °C.

Characterization of BDD electrodes

The surface morphology and grain size of BDD films were analyzed by scanning electron microscopy (SEM). The boron doping and diamond phase purity of BDD films were detected by Raman spectroscopy. The SEM used in this experiment was a Nova Nano SEM 230 field emission scanning electron microscope. The Raman curve was recorded on a LabRAM HR800 laser microscopic Raman spectrometer.

MG electrooxidation

MG was provided by the Chemical Reagent Research Institute of Tianjin, China. Its molecular structure and properties were shown in Table S1 (Supplementary Material). Na_2SO_4, $Na_2S_2O_8$ (analytically pure) were used as experimental supporting electrolytes. Electrooxidation of MG was performed in a 0.5 L container using BDD as anode and stainless steel of 50 mm × 60 mm as the cathode, and the distance between the two electrodes was 6 mm. The magnetic stirrer with a rotating rate of 200 rpm was used during the electrolysis process. All the degradation experiments were performed at room temperature. The degradation efficiency of the dye was tested using an ultraviolet-visible spectrophotometer

(UV-8000S, Metash, Shanghai). The absorbance at the maximum absorption wavelength in the visible region was recorded. The amount of change in solution TOC during the degradation was tested using Shimadzu's TOC analyzer. The color removal and TOC removal were calculated by the following Equation (1) (Martínez-Huitle & Brillas 2009):

$$\text{Removal} = (A_0 - A_t)/A_0 \times 100 \quad (1)$$

The initial absorbance or TOC of the dye and the absorbance or TOC at the time of degradation t is expressed as A_0 and A_t, respectively.

Energy consumption:

$$EC(kWh \cdot m^{-3}) = \frac{E_{cell} It}{V_s} \quad (2)$$

where E_{cell} is the average voltage during electrochemical degradation, the unit is (V); I is the current value in the degradation process, the unit is (A); t is the degradation time, the unit is (h); Vs is malachite green wastewater volume in L.

RESULTS AND DISCUSSION

Characterization of the BDD electrode

The SEM and Raman of the BDD electrode are shown in Figure 1. The diamond have high sp^3/sp^2 ratio due to Raman curve does not show obvious peaks around 1,580 cm^{-1} (sp^2) (Zhang *et al.* 2020), and the characteristic peaks of boron doping are found around 500 cm^{-1} and 1,220 cm^{-1} (Zhang *et al.* 2019). As illustrated in Figure 1(b), the diamond size distribution is uniform, and the particle size distribution is 3–5 μm.

Effect of electro-activated persulfate

The MG removal rate by electro-activated persulfate oxidation is summarized in Figure 2. The color removal rate presents a trend that BDD-EAP > PS > BDD-EO (Figure 2(a)). The color removal rate of BDD-EAP was 95.92% after 30 min, which increased by 3.37 times compared to BDD-EO (28.46%) and 1.80 times compared to PS (53.24%). The TOC removal of BDD-EAP increases by 2.2 times for BDD-EO and 1.7 times for PS at 120 min (Figure 2(b)). This might be the lower yield of $\cdot SO_4^-$ produced by persulfate activation leading to weaker degradation efficiency at room temperature.

In BDD-EAP, the electro-activation of persulfate can occur in both the cathode and anode. As seen in Equations (3) and (4). Persulfate will produce strong oxidizing substances, since $S_2O_8^{2-}$ ($E^0 = 2.01$ V) is electrically activated by the BDD electrode to $\cdot SO_4^-$ ($E^0 = 2.7$ V, SHE). Besides, as seen in Equations (5) and (6), the persulfate has a non-radical oxidation process on the surface of BDD anode to produce transition state HSO_5^-. According to Song (Song *et al.* 2018), pollutants in water are removed by both radical oxidation and non-radical oxidation. The radical oxidation mechanism is dominant for BDD-EAP (Farhat *et al.* 2015). The improvement of MG degradation efficiency under the combined effect:

$$S_2O_8^{2-} + e^- \rightarrow \cdot SO_4^- + SO_4^{2-} \quad (3)$$

$$\cdot SO_4^- + \text{MG} \rightarrow \text{products} \quad (4)$$

$$\cdot SO_4^- + \cdot OH \rightarrow HSO_5^- \quad (5)$$

$$2 \cdot OH \rightarrow H_2O_2 \quad (6)$$

Besides, further investigation of BDD-EAP removal for MG was analyzed by UV-Vis (Figure S1(a)) (Supplementary Material). The characteristic wavelength absorbance peaks

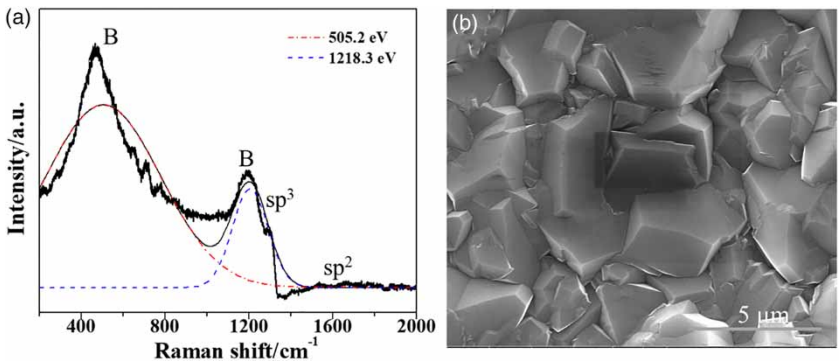

Figure 1 | Characterization of the BDD electrode: (a) electrode Raman diagram and; (b) SEM image of BDD electrode.

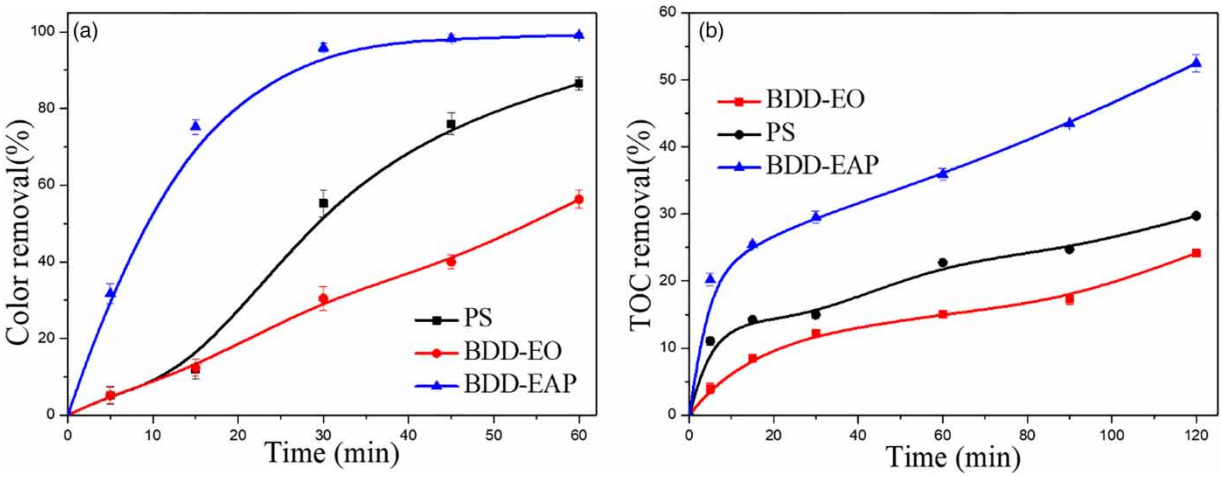

Figure 2 | (a) Color removal rate of MG in PS, BDD-EO and BDD-EAP; (b) TOC removal rate of MG in PS, BDD-EO and BDD-EAP. Other test conditions: pH 4.4; temperature 20 °C.

of MG are located at 315 nm, 425 nm and 618 nm. It should be noted that there is a blue-shift of maximum absorption peak from 617 nm to 604 nm due to the N-demethylation reaction caused by sulfate radical (Liang *et al.* 2017). The damage of the MG conjugate breakage of the whole conjugated aromatic structure can be reflected by the peak drop at 425 nm (Ansari & Nematollahi 2018). The removal rate of the chromophore in the MG can be reflected by the absorbance in the UV-Vis spectrum at 604 nm. It is important to note that there is a new absorption peak at 300 nm, possibly attributed to the benzene ring-opening or the cleavage of central carbon (Liang *et al.* 2017). As shown in Figure S1(b), the intensity of the mark benzene ring at 300 nm is not lowered after the PS addition until 17 h and 70 h. It indicates that the generated degradation byproducts are recalcitrant to persulfate radicals due to the oxidizing ability of persulfate is lower than sulfate radical. Figure S1(c) shows the removal rate of the PS is close to the intensity of BDD-PS at 604 nm. However, it can be seen from UV-Vis spectra that the intensity at 425 nm reflecting the conjugated structure of MG and the intensity at 300 nm indicating the structure of the benzene ring is still high. The chromophore of MG is destroyed by the attack of persulfate, but the conjugated structure and the benzene ring are still unable to be effectively destroyed. This result showed that the BDD-EAP can effectively improve the efficiency of persulfate degradation, and the performance is significantly better than the BDD-EO degradation system.

Effect of electrolyte

The removal of the MG in two electrolytes is shown in Figure 3. The color removal rate for Na_2SO_4 reached 48.90% at 60 min, whereas the color removal for persulfate reached 99.68%. The color removal rate of the persulfate electrolyte was more than 90% at 45 min, which was two times that of sulfate electrolyte. The unit energy consumption is very important for practical application. The unit energy consumption of the persulfate electrolyte is significantly lower than that of the sulfate electrolyte for color removal (Figure 3(b)). As indicated in Figure 3(c), TOC removal increased from 28% (sulfate) to 52% (persulfate). The higher degradation efficiency for persulfate electrolyte than that of sulfate electrolyte due to the half-life of the $\cdot SO_4^-$ with 30–40 μs is usually longer than that of the ·OH (<1 μs), and thus $\cdot SO_4^-$ has better mass transfer performance and contact chance with the target pollutants (Zhi *et al.* 2020). Besides, persulfate electrolyte can significantly reduce the unit energy consumption for TOC removal (Figure 3(d)). The energy consumption of TOC for persulfate electrolyte is a remarkable decrease compared with the sulfate electrolyte. These experimental phenomena indicate that the BDD-EAP not only improves the removal efficiency but also reduces energy consumption.

Effect of persulfate concentration

As indicated above, the electrochemical oxidation of a single organic pollutant can be described by a first-order kinetic model. In this part, the effect of persulfate concentration on MG degradation efficiency was explored, and the first-order kinetic model was plotted to analyze the effect of persulfate concentration on the MG removal efficiency.

As illustrated in Figure 4(a), the color removal for persulfate (PS) of 0.02 M, 0.06 M and 0.1 M reached 99.68%,

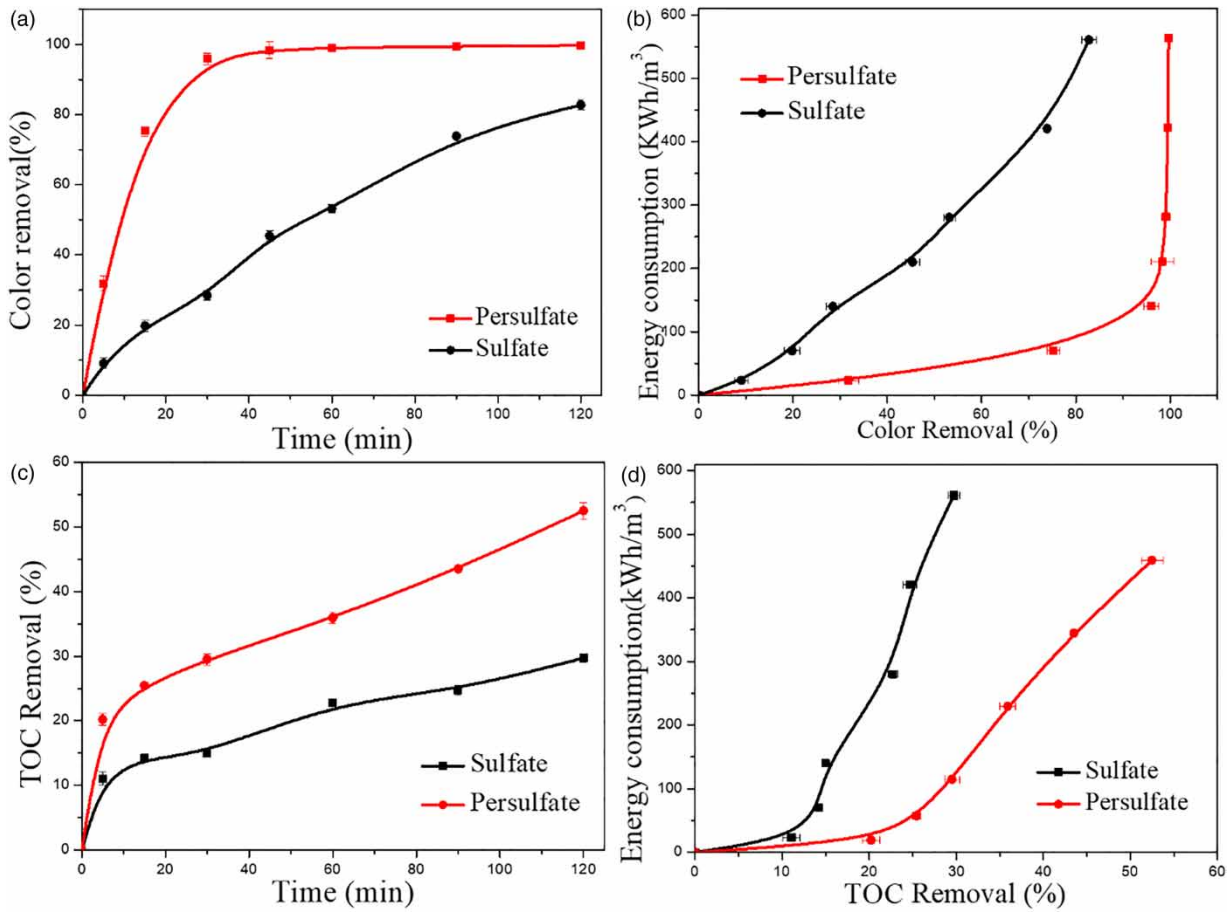

Figure 3 | (a) Color removal rate of MG in sulfate and persulfate; (b) energy consumption versus color removal; (c) TOC removal versus time; (d) energy consumption versus TOC removal. Other test conditions: pH 4.4; temperature 20 °C.

99.93% and 99.75%, respectively. The energy consumption required to remove unit color decreases as the persulfate concentration increases (Figure 4(b)). A control experiment with sulfate as supporting electrolyte to verify the excellent degradation efficiency of BDD-EAP. As shown in Figure S2(a), the color removal rate for Na_2SO_4 of 0.02 M, 0.06 M, and 0.1 M reached 48.90%, 81.89%, and 61.47% at 120 min, respectively. This indicates that the degradation efficiency is significantly improved with the increase of sulfate electrolyte concentration. As a comparison, persulfate electrolyte can achieve high degradation efficiency at low electrolyte concentrations (Figure S2(c)), the rate constants for persulfate concentration of 0.02 M, 0.04 M, 0.06 M, 0.08 M and 0.1 M are 0.091, 0.131, 0.155, 0.167, and 0.179 min^{-1}, respectively. The TOC removal rate gradually increases with the persulfate concentration increase; this is attributed to the production of $\cdot SO_4^-$ increasing with the increase of persulfate electrolyte concentration (Figure 4(c)). The trend of energy consumption to remove the unit TOC is also consistent with the trend of color removal as Figure 4(d).

Figure 4(e) shown as the change of removal rate for three different concentrations of MG by BDD-EAP process. The dye concentration is increased has little effect for MG removal performance, which all can achieve more than 95% within 30 min. This phenomenon is similar to the work of Mei (Mei *et al.* 2018a), which indicates the BDD-EAP can exert strong ability of degradation within a certain organic concentration range.

Effect of current density

In the electrochemical oxidation system, the degradation performance is correlated with current density intimately. As shown in Figure 5(a), the MG removal efficiency is gradually increased with the increases of electrode current density. Besides, the color removal at the initial stage of degradation (10 min) increased with the increase of current

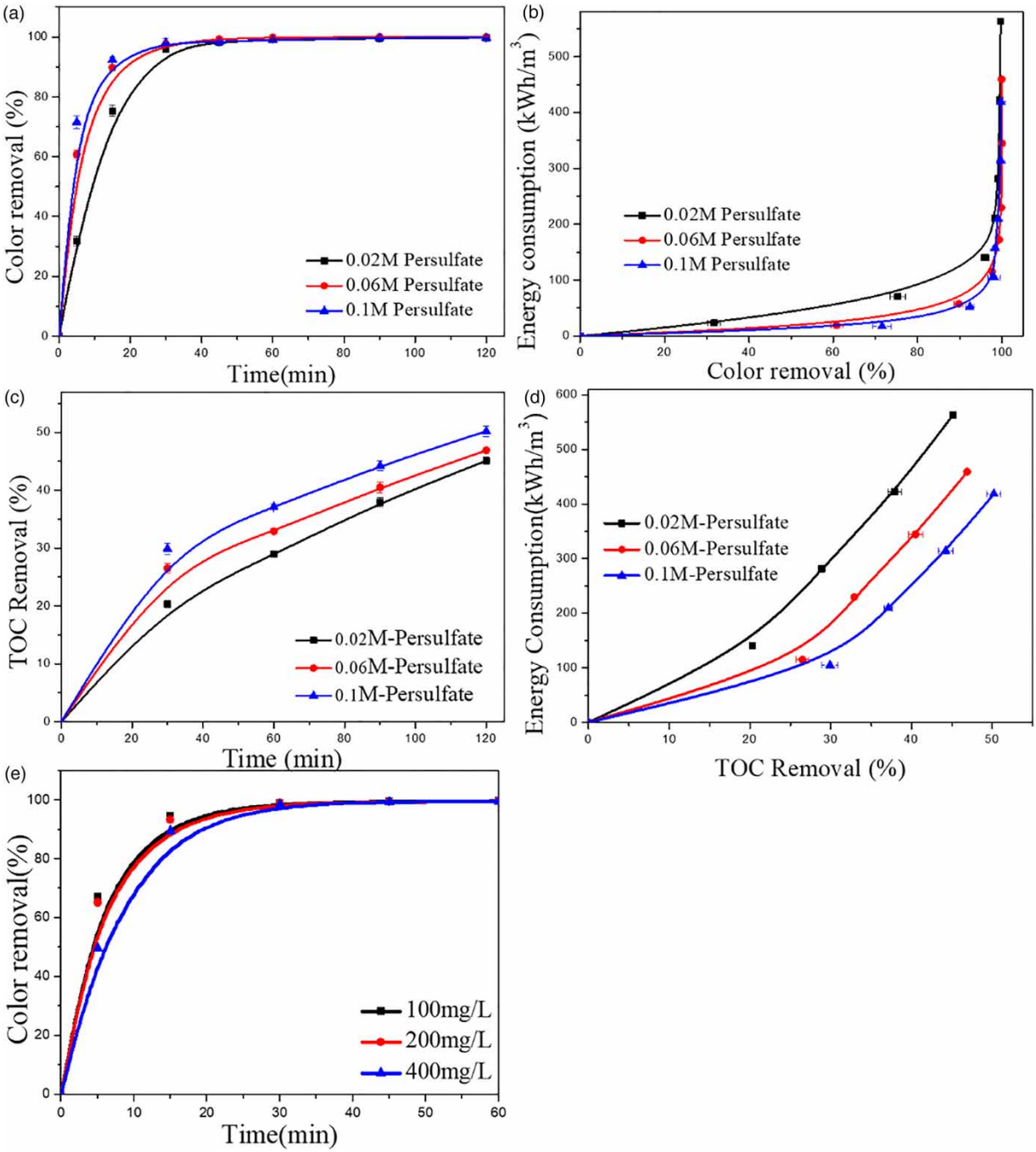

Figure 4 | Effect of persulfate concentrations on MG: (a) color removal with different persulfate concentrations; (b) energy consumption with color removal of persulfate as function; (c) TOC removal with different persulfate concentrations; (d) energy consumption with TOC removal as function; (e) BDD electro-activated persulfate technique to degrade the color removal of MG at a concentration of 100, 200, 400 mg/L. pH 4.4; temperature 20 °C.

density from 1.7 mA/cm^2 (52.40%) to 11.7 mA/(84.82%). The color removal rate with current densities greater than 3.4 mA/cm^2 all exceeded 90% within 15 min. As the kinetic model shows, the degradation rate constants increased from 0.133 to 0.223 min^{-1} with the current density increases, and TOC removal increases from 42.3% to 60.1% (Figure 5(c)). For energy consumption, the unit energy consumption versus TOC removal is rapidly increased with the increase of current density. As seen in Figure 5(a), increasing current density to 5 mA/cm^2 increases significantly the rate of

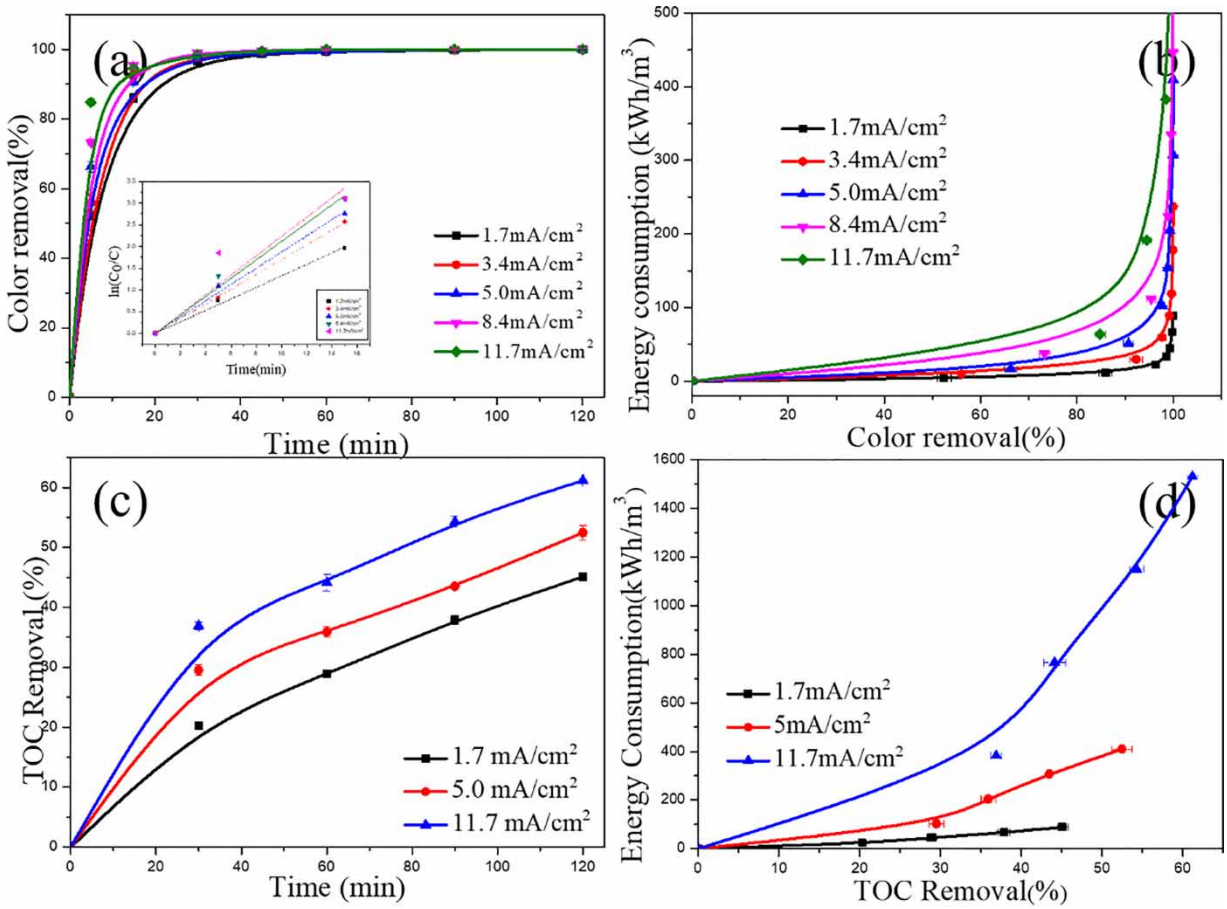

Figure 5 | (a) Color removal of different current densities, the small graph is the kinetic rate constant curve obtained by fitting the initial degradation; (b) Energy consumption versus color removal; (c) TOC removal as function with Time; (d) Energy consumption versus TOC removal. pH 4.4; electrolyte 0.02 M $Na_2S_2O_8$; temperature 20 °C.

MG degradation and has lower energy consumption. Therefore, 5 mA/cm^2 is the optimal current density.

In summary, the increase of current density will lead to the degradation efficiency increasing because it will promote the generation and activation of persulfate. However, the increase of current density will also increase the rate of side reactions, which may lead to the increase in energy consumption and decrease of current efficiency, thereby increasing operating costs.

Effect of pH

The actual type of wastewater is complex, thus with a wide pH range. The ·OH has extremely high sensitivity to the pH of the system. In this paper, the degradation efficiency of MG by BDD-EAP technology for different pH range (2–10) was explored. As shown in Figure 6, the degradation efficiency of the electro-activated persulfate will be affected by the initial pH of water. The degradation efficiency is decreased with the increase of pH (Figure 6(a)). The degradation efficiency is not much different in neutral and weakly alkaline conditions. The same rule can be obtained from the TOC removal rate in Figure 6(b). In traditional hydroxyl radical-based EO process, hydroxyl radicals are unable to maintain high oxidizing power under alkaline pH environments (Haidar *et al.* 2013; Wachter *et al.* 2019). The BDD-EAP technology in this paper can maintain high degradation efficiency in a wide range of pH. The color removal rate all exceeded 87% in pH 2.3–9.8 within 20 min. It is further explained that the technology can suitable for degradation in Widely pH range.

Besides, we compared the degradation efficiency of BDD-EAP and other reported technologies for the electrochemical treatment of MG in Table 1 (El-Ghenymy *et al.* 2015; Ansari & Nematollahi 2018; Jiang *et al.* 2018; Ray *et al.* 2018; Ergut *et al.* 2019). BDD electro-activated persulfate technology is more efficient than other technologies, which indicates the proposed BDD-EAP process is more

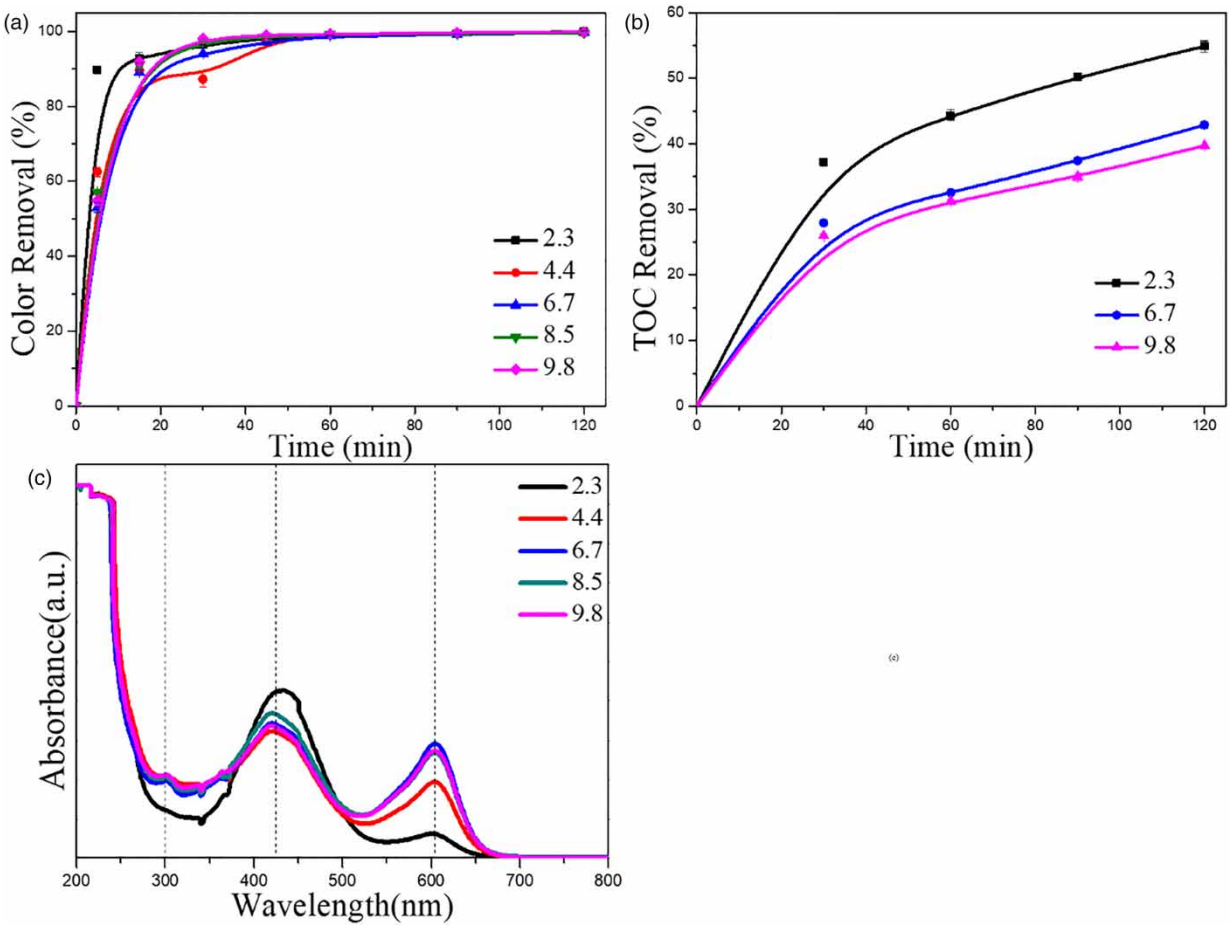

Figure 6 | Effect of initial pH: (a) color removal curve at different pH; (b) TOC removal-Time; (c) UV-Vis spectra of samples of different pH at 15 min. Other test conditions: electrolyte 0.02 M $Na_2S_2O_8$, temperature 20 °C.

Table 1 | Comparison between electro-activated persulfate with other technologies

		Degradation conditions				
Technology	**Dyes**	***j* (mAcm^{-2})**	**C_{dye}**	***T*(°C)**	**Degradation efficiency**	**Reference**
BDD + PS	Malachite green	1.7	400 mgL^{-1}	RT	30 min 98.54%CR	This paper
Photo-Fenton	Malachite green	–	20 mgL^{-1}	RT	60 min 100%CR	Ansari & Nematollahi (2018)
$NiMoO_4$	Malachite green	–	10 ppm	RT	180 min 88.18%	Jiang *et al.* (2018)
G/β-PbO_2	Malachite green	4.0	360 mgL^{-1}	RT	40 min 99.8%CR	El-Ghenymy *et al.* (2015)
Ti/RuO_2- TiO_2	Malachite green	16.9	150 mgL^{-1}	RT	140 min 99%CR	Ray *et al.* (2018)
Fe(III) + H_2O_2	Malachite green	–	10 mM	RT	90 min 83.07%CR	Ergut *et al.* (2019)
AO-SS-BDD	Malachite green	33.3	177 mgL^{-1}	RT	90 min 100%CR	Ray *et al.* (2018)

Where C_{dye}: the initial concentration of dye; RT: room temperature.

privileged in practical application, and in comparison with other related works of BDD-EAP. Song and colleagues (Song *et al.* 2017) used Ti/Pt activated persulfate to degrade organic matter, the changed law of degradation efficiency at pH 1–7 was explored. In this paper, degradation efficiency was measured over a wider pH range (2–10). Frontistis and colleagues (Frontistis *et al.* 2018) reports the law of BDD-EAP degradation of ampicillin by different current

densities (5–110 mA/cm^2). In order to reduce energy consumption, this paper explores the efficient degradation of BDD-EAP at low current density (1.7–11.7 mA/cm^2). Compared with Zhang and colleagues (Zhang *et al.* 2014), this paper investigates the degradation efficiency within a wider range of persulfate (0.02–0.1 M) concentration.

CONCLUSIONS

In this paper, BDD electro-activated persulfate degradation technology is proposed to degrade MG dye organic pollutants. The relationship between persulfate concentration, current density, initial degradation of pH and degradation efficiency are investigated in this paper. The corresponding results indicated this technology possesses the advantages of low energy consumption and high efficiency in a wide pH range, which indicates the proposed BDD-EAP technology is privileged for practical refractory wastewater treatment.

ACKNOWLEDGEMENTS

We gratefully acknowledge the National Key Research and Development Program of China (No. 2016YFB0301402, No. 2016YFB0402705), the National Natural Science Foundation of China (No. 51601226, No. 51874370, No. 51302173), the State Key Laboratory of Powder Metallurgy, the Fundamental Research Funds for the Central Universities of Central South University (2018zzts014 and 2017gczd024), Hunan Provincial Innovation Foundation for Postgraduate (CX2018B085) and the Open-End Fund for Valuable and Precision Instruments of Central South University for financial support.

SUPPLEMENTARY MATERIAL

The Supplementary Material for this paper is available online at https://dx.doi.org/10.2166/wst.2020.176.

REFERENCES

Anglada, A., Urtiaga, A., Ortiz, I., Mantzavinos, D. & Diamadopoulos, E. 2011 Boron-doped diamond anodic treatment of landfill leachate: evaluation of operating variables and formation of oxidation by-products. *Water Research* **45** (2), 828–838.

Ansari, A. & Nematollahi, D. 2018 A comprehensive study on the electrocatalytic degradation, electrochemical behavior and degradation mechanism of malachite green using electrodeposited nanostructured beta-PbO_2 electrodes. *Water Research* **144**, 462–473.

Cai, C., Zhang, H., Zhong, X. & Hou, L. 2014 Electrochemical enhanced heterogeneous activation of peroxydisulfate by Fe-Co/SBA-15 catalyst for the degradation of Orange II in water. *Water Research* **66C**, 473–485.

Candia-Onfray, C., Espinoza, N., Sabino da Silva, E. B., Toledo-Neira, C., Espinoza, L. C., Santander, R., Garcia, V. & Salazar, R. 2018 Treatment of winery wastewater by anodic oxidation using BDD electrode. *Chemosphere* **206**, 709–717.

Cao, M., Hou, Y., Zhang, E., Tu, S. & Xiong, S. 2019 Ascorbic acid induced activation of persulfate for pentachlorophenol degradation. *Chemosphere* **229**, 200–205.

Carter, K. & Farrell, J. 2008 Oxidative destruction of perfluorooctane sulfonate using boron-doped diamond film electrodes. *Environmental Science & Technology* **42**, 6111–6115.

Chaplin, B. P. 2014 Critical review of electrochemical advanced oxidation processes for water treatment applications. *Environmental Science: Processes & Impacts* **16** (6), 1182–1203.

Chen, L., Hu, X., Cai, T., Yang, Y., Zhao, R., Liu, C., Li, A. & Jiang, C. 2019a Degradation of Triclosan in soils by thermally activated persulfate under conditions representative of in situ chemical oxidation (ISCO). *Chemical Engineering Journal* **369**, 344–352.

Chen, Y., Chen, H., Li, J. & Xiao, L. 2019b Rapid and efficient activated sludge treatment by electro-Fenton oxidation. *Water Research* **152**, 181–190.

Deng, Z., Long, H., Wei, Q., Yu, Z., Zhou, B., Wang, Y., Zhang, L., Li, S., Ma, L., Xie, Y. & Min, J. 2017 High-performance non-enzymatic glucose sensor based on nickel-microcrystalline graphite-boron doped diamond complex electrode. *Sensors and Actuators B: Chemical* **242**, 825–834.

Diaz, V., Ibanez, R., Gomez, P., Urtiaga, A. M. & Ortiz, I. 2011 Kinetics of electro-oxidation of ammonia-N, nitrites and COD from a recirculating aquaculture saline water system using BDD anodes. *Water Research* **45** (1), 125–134.

Ding, J., Bu, L., Zhao, Q., Kabutey, F. T., Wei, L. & Dionysiou, D. D. 2019 Electrochemical activation of persulfate on BDD and DSA anodes: electrolyte influence, kinetics and mechanisms in the degradation of bisphenol A. *Journal of Hazardous Materials* **388**, 121789.

El-Ghenymy, A., Centellas, F., Rodríguez, R. M., Cabot, P. L., Garrido, J. A., Sirés, I. & Brillas, E. 2015 Comparative use of anodic oxidation, electro-Fenton and photoelectro-Fenton with Pt or boron-doped diamond anode to decolorize and mineralize Malachite Green oxalate dye. *Electrochimica Acta* **182**, 247–256.

Ergut, M., Uzunoglu, D. & Ozer, A. 2019 Efficient decolourization of malachite green with biosynthesized iron oxide nanoparticles loaded carbonated hydroxyapatite as a reusable heterogeneous Fenton-like catalyst. *Journal of*

Environmental Science and Health, Part A: Toxic/Hazardous Substances & Environmental Engineering **54** (8), 786–800.

Farhat, A., Keller, J., Tait, S. & Radjenovic, J. 2015 Removal of persistent organic contaminants by electrochemically activated sulfate. *Environmental Science & Technology* **49** (24), 14326–14333.

Fernandes, A., Santos, D., Pacheco, M. J., Ciríaco, L. & Lopes, A. 2014 Nitrogen and organic load removal from sanitary landfill leachates by anodic oxidation at Ti/Pt/PbO_2, Ti/Pt/SnO_2-Sb_2O_4 and Si/BDD. *Applied Catalysis B: Environmental* **148–149**, 288–294.

Flores, N., Sirés, I., Rodríguez, R. M., Centellas, F., Cabot, P. L., Garrido, J. A. & Brillas, E. 2017 Removal of 4-hydroxyphenylacetic acid from aqueous medium by electrochemical oxidation with a BDD anode: mineralization, kinetics and oxidation products. *Journal of Electroanalytical Chemistry* **793**, 58–65.

Frontistis, Z., Mantzavinos, D. & Meric, S. 2018 Degradation of antibiotic ampicillin on boron-doped diamond anode using the combined electrochemical oxidation – sodium persulfate process. *Journal of Environmental Management* **223**, 878–887.

Gao, Y.-q., Gao, N.-y., Chu, W.-h., Zhang, Y.-f., Zhang, J. & Yin, D.-q. 2019 UV-activated persulfate oxidation of sulfamethoxypyridazine: kinetics, degradation pathways and impact on DBP formation during subsequent chlorination. *Chemical Engineering Journal* **370**, 706–715.

García-Rodríguez, O., Bañuelos, J. A., El-Ghenymy, A., Godínez, L. A., Brillas, E. & Rodríguez-Valadez, F. J. 2016 Use of a carbon felt–iron oxide air-diffusion cathode for the mineralization of Malachite Green dye by heterogeneous electro-Fenton and UVA photoelectro-Fenton processes. *Journal of Electroanalytical Chemistry* **767**, 40–48.

Gopinathan, R., Kanhere, J. & Banerjee, J. 2015 Effect of malachite green toxicity on non target soil organisms. *Chemosphere* **120**, 637–644.

Guenfoud, F., Mokhtari, M. & Akrout, H. 2014 Electrochemical degradation of malachite green with BDD electrodes: effect of electrochemical parameters. *Diamond and Related Materials* **46**, 8–14.

Haidar, M., Dirany, A., Sires, I., Oturan, N. & Oturan, M. A. 2013 Electrochemical degradation of the antibiotic sulfachloropyridazine by hydroxyl radicals generated at a BDD anode. *Chemosphere* **91** (9), 1304–1309.

Hayat, W., Zhang, Y., Hussain, I., Du, X., Du, M., Yao, C., Huang, S. & Si, F. 2019 Efficient degradation of imidacloprid in water through iron activated sodium persulfate. *Chemical Engineering Journal* **370**, 1169–1180.

He, Y., Huang, W., Chen, R., Zhang, W. & Lin, H. 2015 Improved electrochemical performance of boron-doped diamond electrode depending on the structure of titanium substrate. *Journal of Electroanalytical Chemistry* **758**, 170–177.

Jiang, D. B., Liu, X., Xu, X. & Zhang, Y. X. 2018 Double-shell Fe_2O_3 hollow box-like structure for enhanced photo-Fenton degradation of malachite green dye. *Journal of Physics and Chemistry of Solids* **112**, 209–215.

Katsoni, A., Mantzavinos, D. & Diamadopoulos, E. 2014 Sequential treatment of diluted olive pomace leachate by digestion in a pilot scale UASB reactor and BDD electrochemical oxidation. *Water Research* **57**, 76–86.

Liang, S. X., Jia, Z., Zhang, W. C., Wang, W. M. & Zhang, L. C. 2017 Rapid malachite green degradation using Fe73.5Si13.5B9Cu1Nb3 metallic glass for activation of persulfate under UV–Vis light. *Materials & Design* **119**, 244–253.

Lin, X., Ma, Y., Wan, J., Wang, Y. & Li, Y. 2019 Efficient degradation of Orange G with persulfate activated by recyclable $FeMoO_4$. *Chemosphere* **214**, 642–650.

Long, Y., Feng, Y., Li, X., Suo, N., Chen, H., Wang, Z. & Yu, Y. 2019 Removal of diclofenac by three-dimensional electro-Fenton-persulfate (3D electro-Fenton-PS). *Chemosphere* **219**, 1024–1031.

Martínez-Huitle, C. A. & Brillas, E. 2009 Decontamination of wastewaters containing synthetic organic dyes by electrochemical methods: a general review. *Applied Catalysis B: Environmental* **87** (3–4), 105–145.

Matzek, L. W. & Carter, K. E. 2016 Activated persulfate for organic chemical degradation: a review. *Chemosphere* **151**, 178–188.

Mei, R., Zhu, C., Wei, Q., Ma, L., Li, W., Zhou, B., Deng, Z., Tong, Z., Ouyang, G. & Jiang, C. 2018a The dependence of oxidation parameters and dyes' molecular structures on microstructure of boron-doped diamond in electrochemical oxidation process of dye wastewater. *Journal of The Electrochemical Society* **165** (7), H324–HH32.

Mei, X., Wei, Q., Long, H., Yu, Z., Deng, Z., Meng, L., Wang, J., Luo, J., Lin, C.-T., Ma, L., Zheng, K. & Hu, N. 2018b Long-term stability of Au nanoparticle-anchored porous boron-doped diamond hybrid electrode for enhanced dopamine detection. *Electrochimica Acta* **271**, 84–91.

Mei, R., Wei, Q., Zhu, C., Ye, W., Zhou, B., Ma, L., Yu, Z. & Zhou, K. 2019 3D macroporous boron-doped diamond electrode with interconnected liquid flow channels: a high-efficiency electrochemical degradation of RB-19 dye wastewater under low current. *Applied Catalysis B: Environmental* **245**, 420–427.

Perez-Estrada, L. A., Aguera, A., Hernando, M. D., Malato, S. & Fernandez-Alba, A. R. 2008 Photodegradation of malachite green under natural sunlight irradiation: kinetic and toxicity of the transformation products. *Chemosphere* **70** (11), 2068–2075.

Qu, W., Yuan, T., Yin, G., Xu, S., Zhang, Q. & Su, H. 2019 Effect of properties of activated carbon on malachite green adsorption. *Fuel* **249**, 45–53.

Ray, S. K., Dhakal, D. & Lee, S. W. 2018 Insight into malachite green degradation, mechanism and pathways by morphology-tuned alpha-$NiMoO_4$ photocatalyst. *Photochemistry and Photobiology* **94** (3), 552–563.

Sasidharan Pillai, I. M. & Gupta, A. K. 2016 Effect of inorganic anions and oxidizing agents on electrochemical oxidation of methyl orange, malachite green and 2,4-dinitrophenol. *Journal of Electroanalytical Chemistry* **762**, 66–72.

Siedlecka, E. M., Ofiarska, A., Borzyszkowska, A. F., Bialk-Bielinska, A., Stepnowski, P. & Pieczynska, A. 2018 Cytostatic drug removal using electrochemical oxidation

with BDD electrode: degradation pathway and toxicity. *Water Research* **144**, 235–245.

Song, H., Yan, L., Ma, J., Jiang, J., Cai, G., Zhang, W., Zhang, Z., Zhang, J. & Yang, T. 2017 Nonradical oxidation from electrochemical activation of peroxydisulfate at Ti/Pt anode: efficiency, mechanism and influencing factors. *Water Research* **116**, 182–193.

Song, H., Yan, L., Jiang, J., Ma, J., Zhang, Z., Zhang, J., Liu, P. & Yang, T. 2018 Electrochemical activation of persulfates at BDD anode: radical or nonradical oxidation? *Water Research* **128**, 393–401.

Srivastava, S., Sinha, R. & Roy, D. 2004 Toxicological effects of malachite green. *Aquatic Toxicology* **66** (3), 319–329.

Su, S., Liu, Y., He, W., Tang, X., Jin, W. & Zhao, Y. 2019 A novel graphene oxide-carbon nanotubes anchored alpha-FeOOH hybrid activated persulfate system for enhanced degradation of Orange II. *Journal of Environmental Sciences (China)* **83**, 73–84.

Sun, J., Chen, Y., Xiang, Y., Ling, L., Fang, J. & Shang, C. 2019 Oxidative debromination of 2,2-bis(bromomethyl)-1,3-propanediol by UV/persulfate process and corresponding formation of brominated by-products. *Chemosphere* **228**, 735–743.

Taner Can, O., Bayramoglu, M., Sozbir, M. & Aras, O. 2019 Mineralization of o-tolidine by electrooxidation with BDD, Ti/Pt and MMO anodes. *Desalination and Water Treatment* **141**, 377–385.

Wachter, N., Aquino, J. M., Denadai, M., Barreiro, J. C., Silva, A. J., Cass, Q. B., Bocchi, N. & Rocha-Filho, R. C. 2019 Electrochemical degradation of the antibiotic ciprofloxacin in a flow reactor using distinct BDD anodes: reaction kinetics, identification and toxicity of the degradation products. *Chemosphere* **234**, 461–470.

Xing, X., Ni, J., Zhu, X., Jiang, Y. & Xia, J. 2018 Maximization of current efficiency for organic pollutants oxidation at BDD, Ti/SnO_2-Sb/PbO_2, and Ti/SnO_2-Sb anodes. *Chemosphere* **205**, 361–368.

Xiong, X., Sun, B., Zhang, J., Gao, N., Shen, J., Li, J. & Guan, X. 2014 Activating persulfate by Fe(0) coupling with weak magnetic field: performance and mechanism. *Water Research* **62**, 53–62.

Zhang, H., Wang, Z., Liu, C., Guo, Y., Shan, N., Meng, C. & Sun, L. 2014 Removal of COD from landfill leachate by an electro/Fe^{2+}/peroxydisulfate process. *Chemical Engineering Journal* **250**, 76–82.

Zhang, L., Zhou, K., Wei, Q., Ma, L., Ye, W., Li, H., Zhou, B., Yu, Z., Lin, C.-T., Luo, J. & Gan, X. 2019 Thermal conductivity enhancement of phase change materials with 3D porous diamond foam for thermal energy storage. *Applied Energy* **233–234**, 208–219.

Zhang, L., Wei, Q., An, J., Ma, L., Zhou, K., Ye, W., Yu, Z., Gan, X., Lin, C.-T. & Luo, J. 2020 Construction of 3D interconnected diamond networks in Al-matrix composite for high-efficiency thermal management. *Chemical Engineering Journal* **380**, 122551.

Zheng, K., Longn, H., Wei, Q., Ma, L., Qiao, L., Li, C., Meng, L., Lin, C.-T., Jiang, Y., Zhao, T. & Zhou, K. 2019 Non-enzymatic glucose sensor based on hierarchical Au/Ni/boron-doped diamond heterostructure electrode for improving performances. *Journal of The Electrochemical Society* **166** (6), B373–BB80.

Zhi, D., Lin, Y., Jiang, L., Zhou, Y., Huang, A., Yang, J. & Luo, L. 2020 Remediation of persistent organic pollutants in aqueous systems by electrochemical activation of persulfates: a review. *Journal of Environmental Management* **260**, 110125.

Zhou, M., Särkkä, H. & Sillanpää, M. 2011 A comparative experimental study on methyl orange degradation by electrochemical oxidation on BDD and MMO electrodes. *Separation and Purification Technology* **78** (3), 290–297.

Zhou, B., Yu, Z., Wei, Q., Long, H., Xie, Y. & Wang, Y. 2016 Electrochemical oxidation of biological pretreated and membrane separated landfill leachate concentrates on boron doped diamond anode. *Applied Surface Science* **377**, 406–415.

Zhu, C., Jiang, C., Chen, S., Mei, R., Wang, X., Cao, J., Ma, L., Zhou, B., Wei, Q., Ouyang, G., Yu, Z. & Zhou, K. 2018 Ultrasound enhanced electrochemical oxidation of Alizarin Red S on boron doped diamond(BDD) anode: effect of degradation process parameters. *Chemosphere* **209**, 685–695.

First received 8 November 2019; accepted in revised form 3 April 2020. Available online 22 April 2020